

Evaluation of Load-Bearing Capacity in Japanese Arch Steel Aqueduct Bridge through Structural Redundancy Assessment

Nima Mohammadi¹

Ph.D. Candidate

Dept. of Civil Eng., Grad. School of Eng.,
Kobe University, Japan

Yasuko Kuwata²

Professor

Dept. of Civil Eng., Grad. School of Eng.,
Kobe University, Japan

Abstract:- Structural redundancy assessment of steel aqueduct bridges is made by the analysis of a case study using the Musota Aqueduct bridge structure: a simply supported steel arch bridge erected in 1973 and a seven-span continuous steel aqueduct bridge. In this paper, as a case study, after the validation of the model, the structural redundancy of the Musota aqueduct bridge in Wakayama City with respect to its load-carrying capacity after the failure of hanging components due to corrosion was investigated. The conventional procedure for the assessment of redundancy makes use of static nonlinear structural analysis. A three-dimensional finite-element model of this bridge was developed to simulate its behavior. The results from the linear analysis are compared with those from the nonlinear analysis to investigate the appropriateness of the former in the evaluation of redundancy. A detailed nonlinear static finite element study is carried out into the hangers' components of the arch bridge in order to clarify the implications involved in the failure of redundancy. Finally, recommendations for prudent bridge maintenance methods are presented based on findings from the investigation.

Keywords:- Redundancy Analysis, Load Capacity, Hangers, Arch Aqueduct Bridge, Damage.

I. INTRODUCTION

Langer arch bridges have historically represented significant achievements in early bridge architecture, with a notable legacy in worldwide infrastructure. Notwithstanding their historical importance, these buildings, like to other civil engineering achievements, are susceptible to a range of unexpected difficulties, such as corrosion, which may severely undermine their stability. Conventional design approaches emphasize load-bearing capabilities in steel bridge construction; nevertheless, the intricate relationship between Langer arch aqueduct bridges and various types of damage, including corrosion, blast events, and seismic stresses, presents a domain of uncharted complications. Until the modern age, academic discussion of the redundancy of aqueduct bridges to such challenges has been significantly restricted, necessitating a more thorough examination of their

structural behavior and response mechanisms. Subsequent to the incident on October 3, 2021, which resulted in the catastrophic failure of the Musota Aqueduct Bridge over the Kinokawa River in Wakayama City, Japan Figure 1 and 2, significant scrutiny has been directed toward the structural integrity of this type of bridge [1], [2], [3].

Previous occurrences of bridge failure have been ascribed to corrosion and structural inadequacies. The collapse of the Mississippi River Bridge on August 1, 2007, in Minneapolis, Minnesota, USA, has sparked considerable interest in examining the structural redundancy of steel truss bridges, hereafter referred to as "redundancy." Redundancy denotes a structural system's capacity to endure a certain degree of residual strength and avert collapse after the breakdown of an individual member or component within the system[4]. The need of ensuring system redundancy was underscored by the disastrous failure of the Minneapolis bridge in 2007 [5]. Structural engineers are concurrently engaged in study and enhancement of cost-effective methods to fortify bridge designs, safeguarding human lives and averting probable structural failures, whether partial or total. Innovative design methodologies that emphasize redundancy and resilience provide significant potential for reducing progressive collapse and enhancing the durability of future bridge projects. Thus, the present research aims to investigate the redundancy of the hanging element in a Langer arch aqueduct bridge and assess the bridge's robustness under standard service loading circumstances.

II. INCIDENT

On October 3, 2021, a significant structural failure occurred with the partial collapse of the Musota aqueduct bridge over the Ki-nokawa River in Wakayama City. The collapse was attributed to the installation of a retrofit member on the hanging member to mitigate wind damage. Nevertheless, the accumulation of dust, water, and guano on the member resulted in corrosion that compromised its integrity, ultimately leading to its fracture. The exact position of the fracture in the suspended part was indeterminate during the examination from the control walkway between the aqueduct bridge's pipes. The fracture occurred in a blind area above the modified components.



Fig 1 Wakayama Aqueduct Bridge Failure

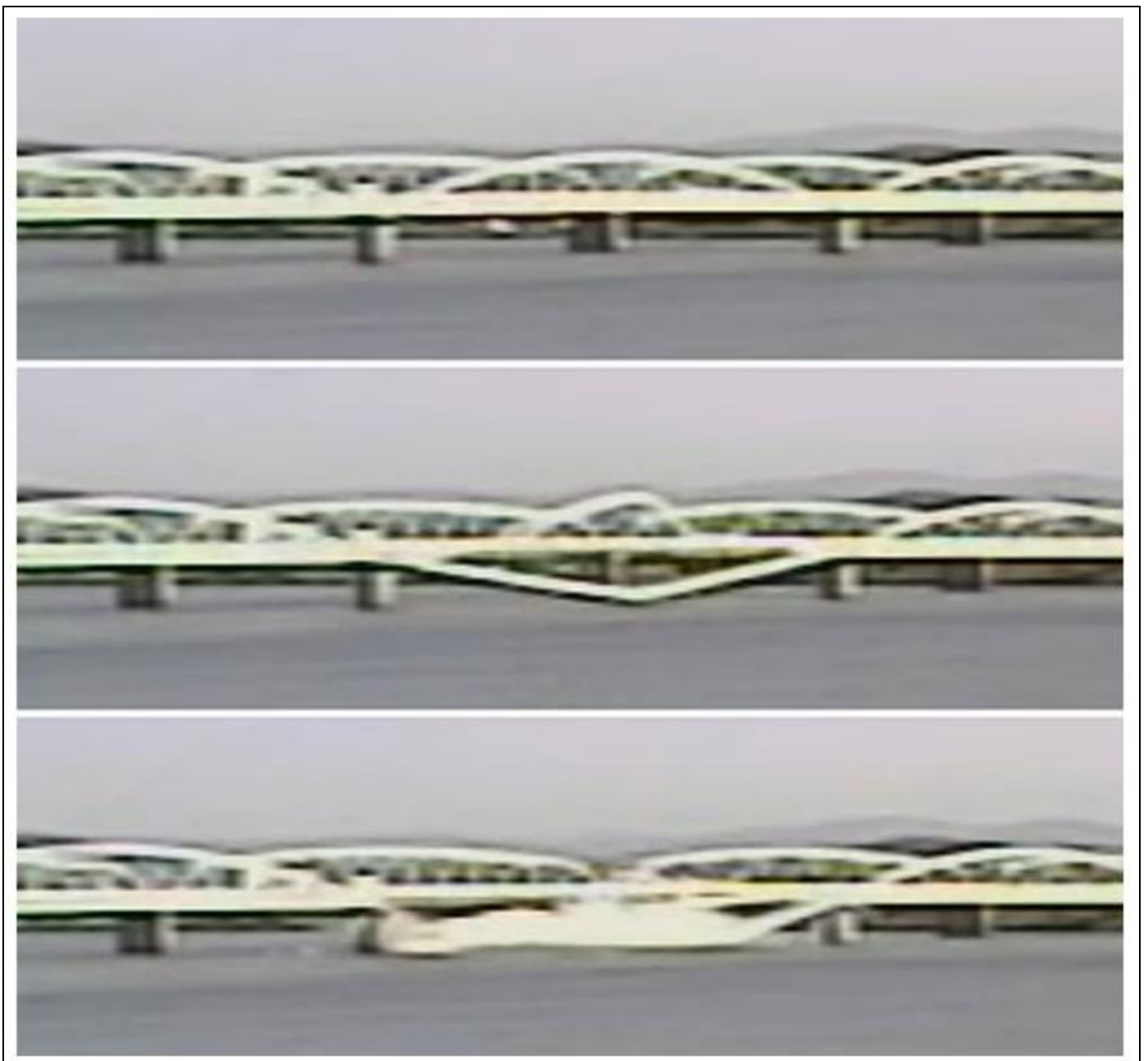


Fig 2 Wakayama Aqueduct Bridge Failure view of a Camera[6]

Within the industrial sector, there is an increased appreciation of the role that aqueducts play in water resource distribution; thus, very strict engineering criteria have been established for such systems. The same awareness is evidenced through the growing literature that stipulates operating standards and provides for the durability of water transportation structures. On one hand, the mechanical behavior of the materials adopted in aqueducts has been widely investigated [7]; [8] have set a representative benchmark for general industrial standards with regard to pipeline durability. However, very few studies have been conducted with regard to the actual performance of an aqueduct after structural repair. Common pipeline repair methods include the insertion of steel liners, and this technique has been highly controversially discussed [9]. Other techniques, such as the application of an external steel sleeve, were critically analyzed by [10], referring to their efficiency in different environmental conditions. Nowadays, FRP has been one of the most valid options for conventional steel material replacement because of its efficiency and rapidness in pipeline rehabilitation. A pioneering research by [11] shows that FRP can extend the service life of existing pipelines with little disruption to operation.

The use of FRP composite materials in rehabilitation methodologies does, therefore, hold a great deal of promise for the rehabilitation requirements of underground piping systems. The attractiveness of FRP composites as construction.

III. REDUNDANCY AND PROGRESSIVE COLLAPSE

Redundancy, sometimes synonymous with alternate load routes, is essential for buildings to spread loads and alleviate localized damage consequences[12]. It depends on alternate load pathways or additional transfer mechanisms to avert abrupt failure in cases of localized damage. Defining redundancy in bridge design or assessment standards is challenging, yet academic literature provides valuable interpretations. Bridge redundancy is defined by some as the capacity to maintain load-bearing functions despite component failure[4], but others interpret it more broadly as the lack of critical components that might result in structural failure[13]. This discussion outlines three forms of redundancy: load-path, structural, and internal redundancy [14].

In steel bridge assemblies, redundancy is linked to the classification of fracture critical elements (FCMs), including hanging members and tension ties in Langer arch bridges, recognized as essential for structural stability [15]. The structural reaction to high dynamic loads, such as seismic and blast loading, is a crucial element of redundancy. The capacity to endure localized damage without failure is essential, especially in mitigating progressive collapse issues[16].

The validation of structural members relied on the use of R values obtained from recognized mathematical equations (Eqs. (1) and (2)). These equations, derived from previous academic research, served as essential tools for evaluating the structural sufficiency of the designated parts. A crucial criteria used in this assessment was identifying the end-of-life status for each individual, signified by achieving an R-value of 1.0 or above. In redundancy analysis, Eq. (1) is used for tensile axial forces, whereas Eq. (2) is employed for compressive axial forces. Reassessing redundancy using Eqs. (1) or (2) that results in a value of 1.0 or above indicates that the section force exceeds the ultimate strength of the section. Equations (1) and (2) function as verification methods within the framework of the limit state design approach.

When an axial force is exerted in tension:

$$R = \left(\frac{P}{P_p} \right) + \left(\frac{M_p}{M_{py}} \right) + \left(\frac{M_z}{M_{pz}} \right) \quad (1)$$

When an axial force is exerted in compression:

$$R = \left(\frac{P}{P_u} \right) + \frac{1}{1 - \left(\frac{P}{P_E} \right)} \left(\frac{M_y}{M_{py}} \right) + \frac{1}{1 - \left(\frac{P}{P_E} \right)} \left(\frac{M_z}{M_{pz}} \right) \quad (2)$$

Where, P , M_y , M_z are working axial force, working moment (in-plane), and working moment (out-plane); P_p , M_{py} , M_{pz} are full plastic axial force, full plastic moment (in-plane), and full plastic moment (out-plane); P_E is Euler's buckling axial force, P_u is ultimate compressive strength in consideration of buckling.

IV. FINITE ELEMENT MODEL

Our work included numerical modeling using Abaqus/CAE 2024 on a high-performance computer machine including 40 processing cores. The material qualities of the pipe, as shown in Table 1, adhered to Grade SS400 criteria, serving as a crucial component of the aqueduct bridge construction. Structural elements such as upper and lower chords, diagonals, transverse and longitudinal girders, lean-to structures, main pipeline, and transverse structures were precisely modeled using beam elements. Meshing was performed with an emphasis on granularity, mostly using beam components to improve model precision. The collapsed bridge, measuring 60.8 meters, surpassed the dimensions of nearby spans and had an extra air valve load at the center, as seen in Figure 3. The aqueduct bridge girder, constructed from a 0.914-meter diameter steel circular pipe, supported two water transmission lines. The mechanical parameters of steel, including a Young's modulus of 200 GPa, a Poisson's ratio of 0.3, and a mass density of 7800 kg/m³, were accurately included into our beam element model with pinned supports.

Table 1 Steel and Bridge Specification

Item	Note
Water pipe diameter	900A (Outer diameter 914.4mm)
Type	Seven-span Langer arch bridges and two-span single-beam bridges
Steel used	STPY 41, STK41, SS41
Bearing	Roller and pin bearings
Span	60.3 m
Young's Modulus	200 GPa
Poisson ratio	0.3
Steel Density	~7800 kg/m ³
Water density	1000 kg/m ³

The Musota Aqueduct Bridge has a unique architectural design with two sets of hanging members supporting each major pipeline, together with vertical hanging members for the aqueduct bridge girder, as seen in Figure 4. The suspended components, similar to the main pipeline, are fabricated from SS400-grade steel. Additionally, the impact of water load was integrated using a simplified model that included a water mass density of 1000 kg/m³ as a loading condition for the pipe. The integration of all steel components in the bridge was carefully performed to guarantee structural integrity and facilitate welding connections. Comprehensive details of the accepted modeling approaches are discussed in separate case studies, clarifying the intricacies of the analytical methodology used. The study includes applied loads, namely the dead load and

living load (water load). Furthermore, instances of corrosion of suspended components that transpired during the Musota aqueduct bridge incident were included for comparison analysis.

Figures 5 and 6 depicts the methods used to calculate the cross-sectional force at the ruptured cases. The study included cross-sectional forces in the undamaged condition of the structure under the effects of dead and live loads, while integrating cross-sectional forces related to the presumed ruptured member in the opposing direction after its removal. This technique enabled a thorough assessment of the structural reaction to the rupture event, including both intact and post-failure conditions of the bridge components.

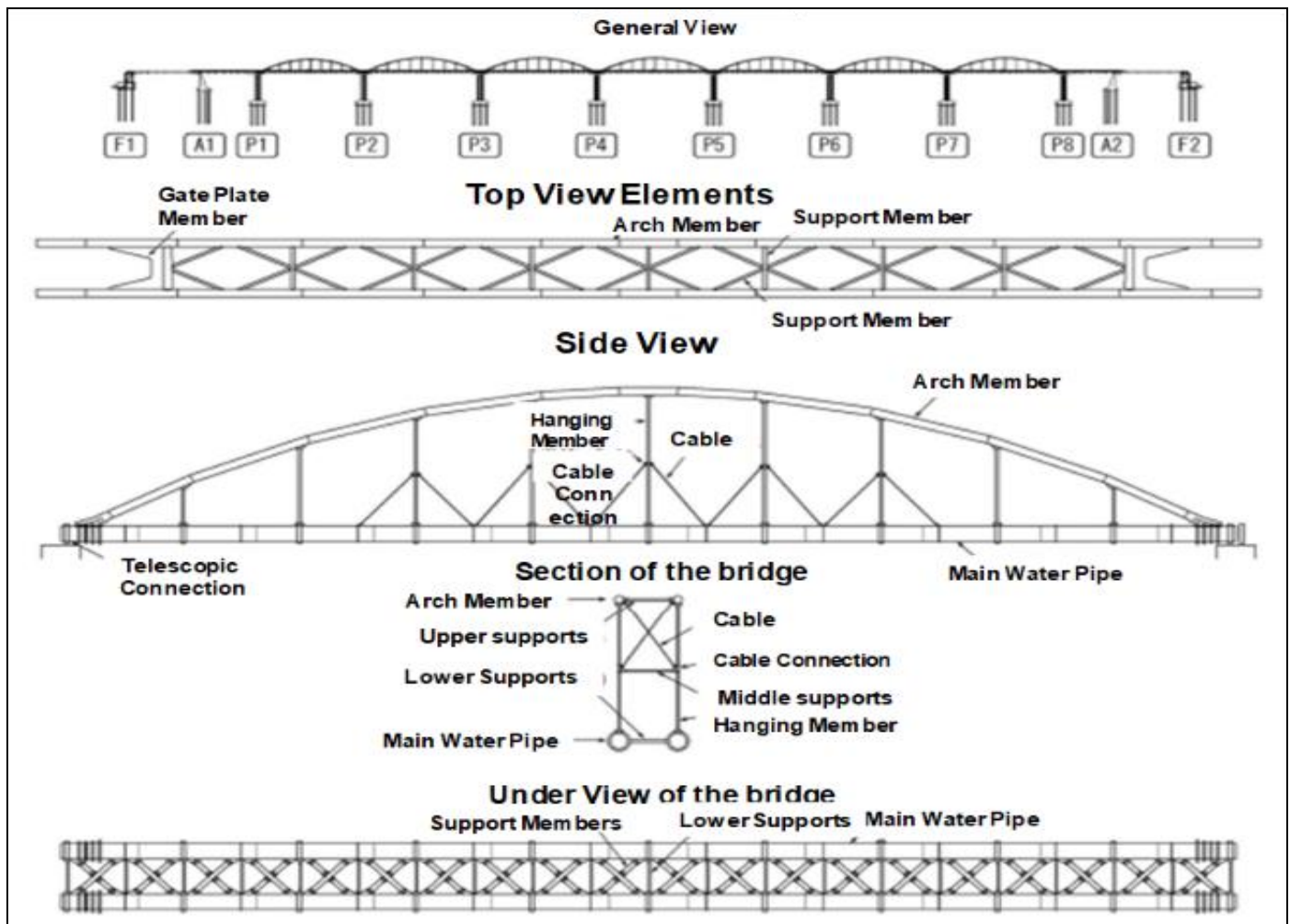


Fig 3 General view of the Bridge and Different Parts

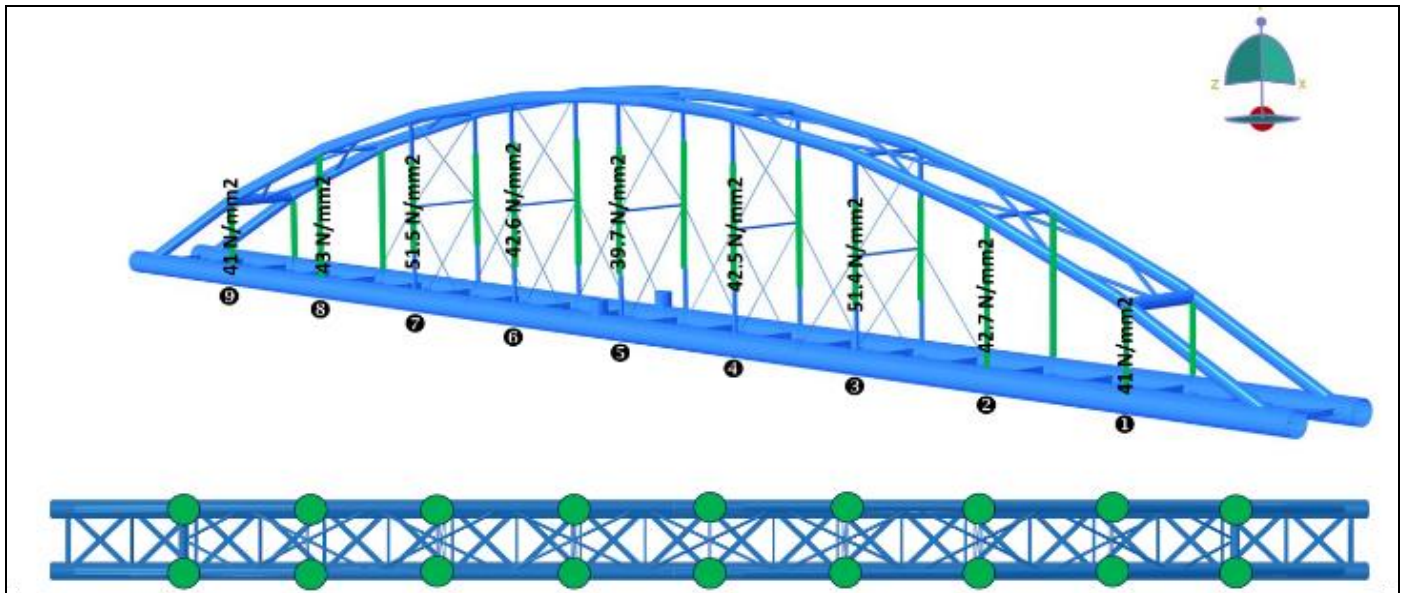
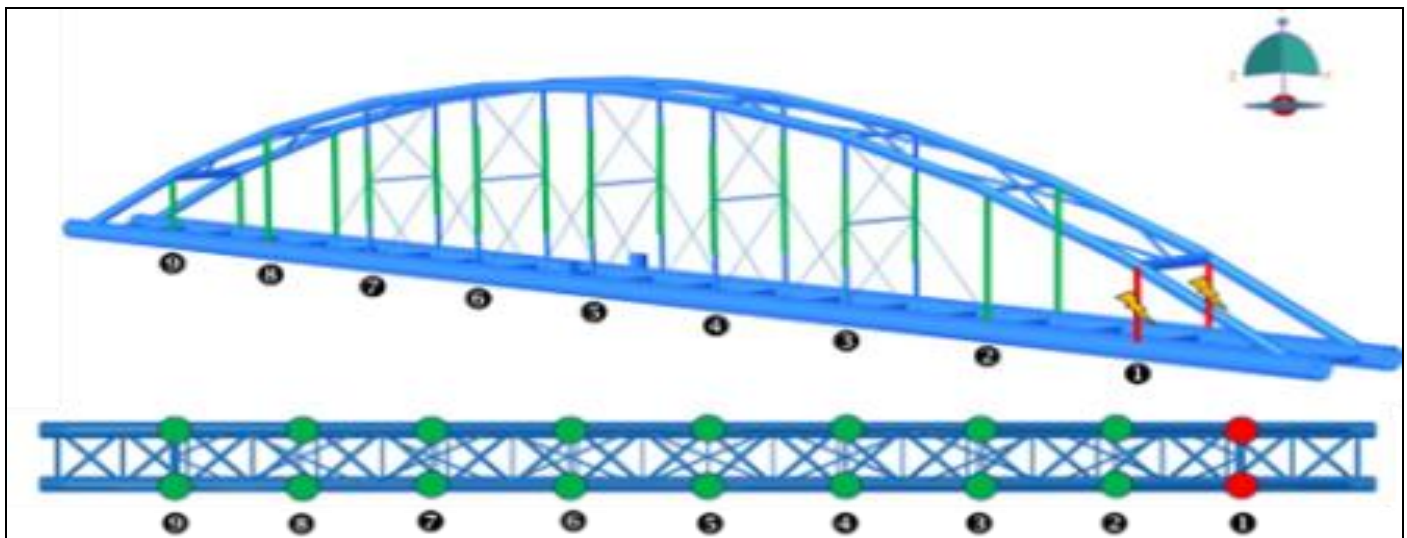
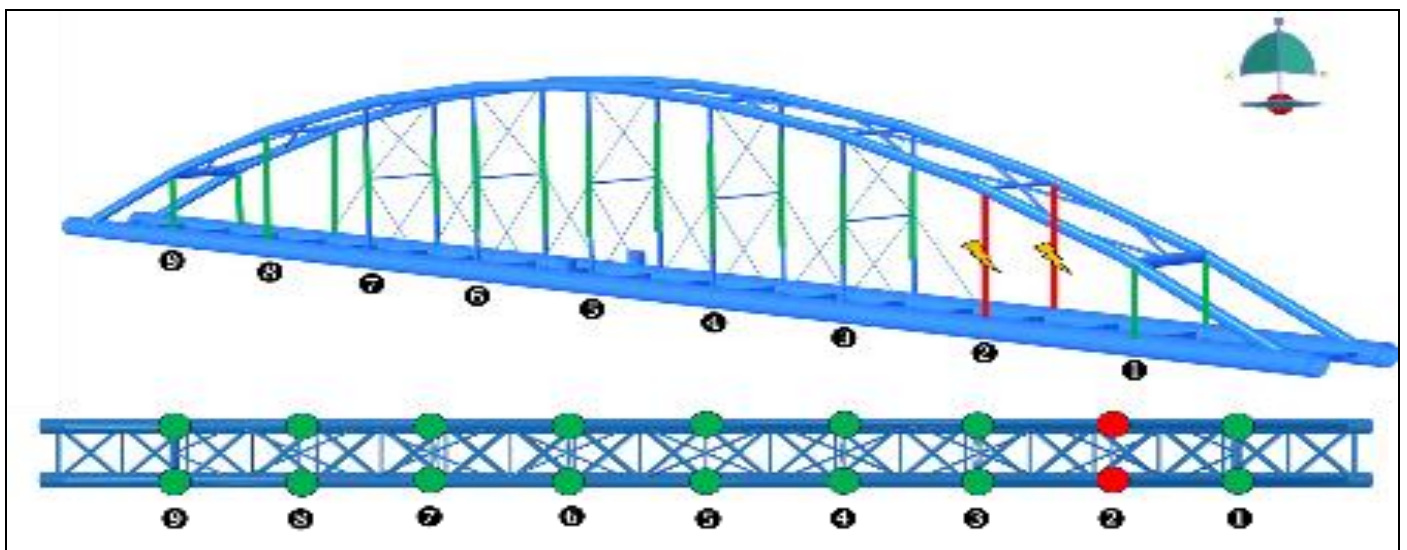


Fig 4 Intact model of Musota Aqueduct Bridge showing the places where the hanging members are intact shown in Green Color

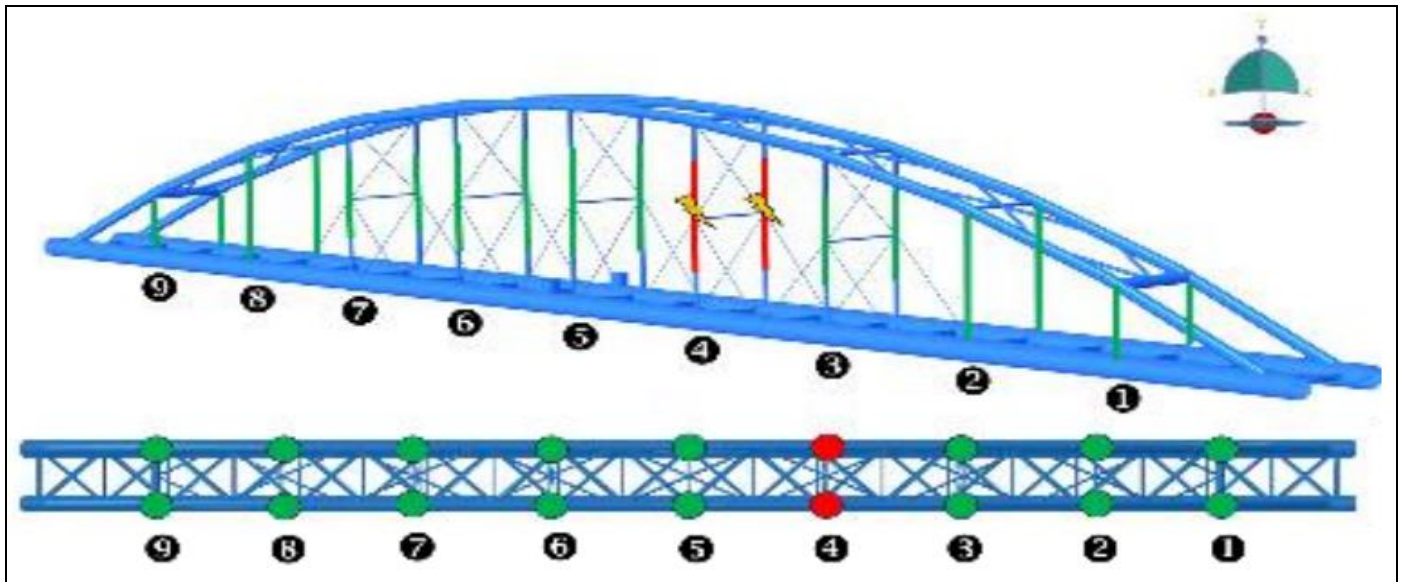


(a)

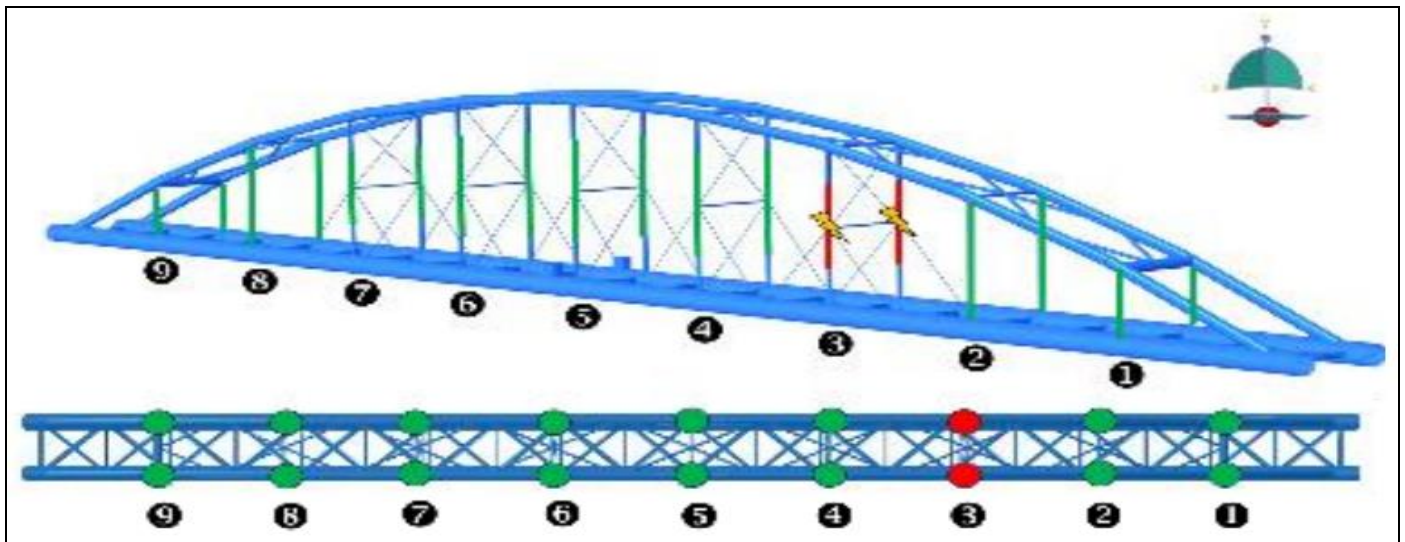


(b)

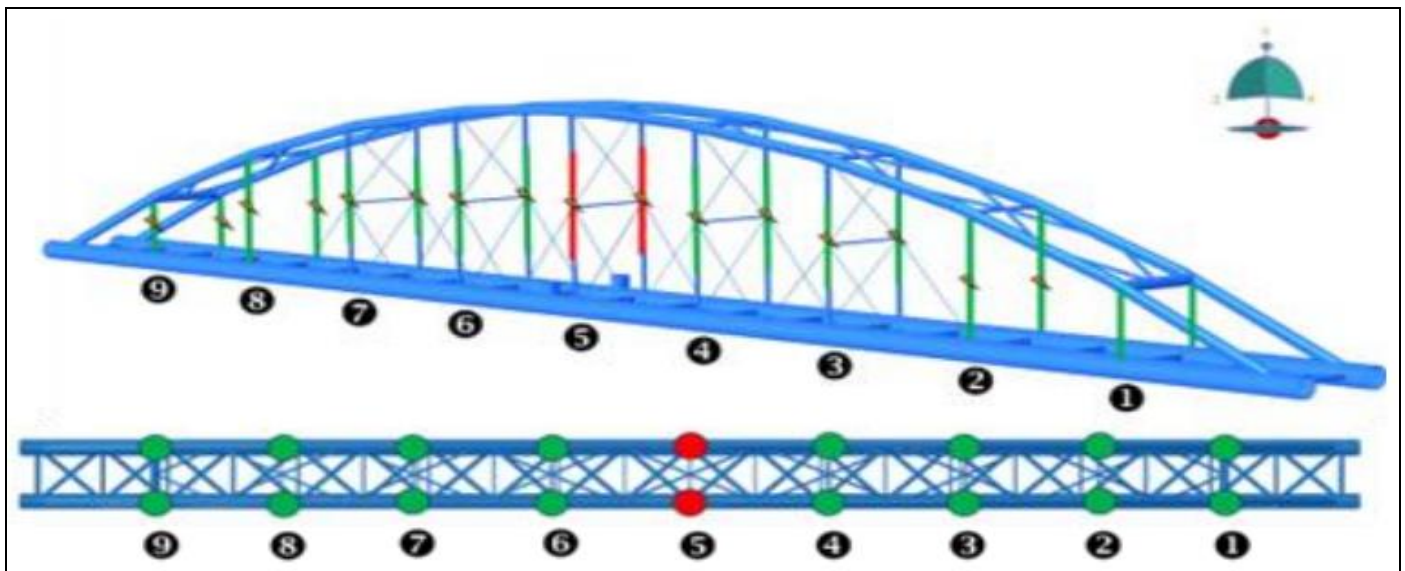
Fig 5 Case Scenarios model of Musota Aqueduct Bridge



(c)



(d)



(e)

Fig 6 Case Scenarios model of Musota Aqueduct Bridge

V. CORROSION

In our investigation into the corrosive effects on structural elements, we utilize various methodologies, including deliberate reduction of material cross-sectional area, which has proven effective in computational models see as Figures 4 to 6. External corrosion, particularly affecting hanging members, is simulated by systematically reducing the cross-sectional area to mimic corrosion-induced material loss. Bird guano exacerbates steel corrosion due to its chemical

composition, rich in uric acid and ammonia, creating a highly acidic environment upon contact with steel surfaces. This acidic environment accelerates the corrosion process by promoting rust formation; Moisture, rain, and bird guano combine to create an electrolytic environment, further enhancing corrosion and structural deterioration. Effective maintenance and cleaning protocols are essential to mitigate the corrosive impact of bird guano on steel infrastructure Figure 7.

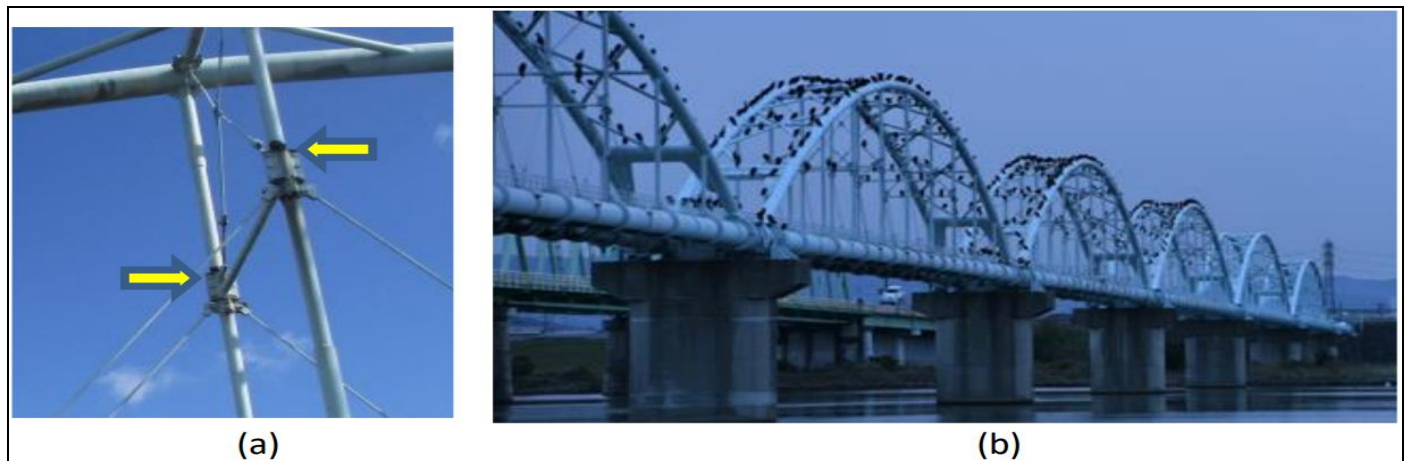


Fig 7 Fracture of hanging member above the window protection member on the P5-P6 span adjacent to the collapsed span (b) birds sitting on the bridge and effect of birds’ guano on the aqueduct bridge.

VI. RESULTS AND DISCUSSION

Modeling of members in the event of material rupture is provided as an illustrative case within the context of redundancy analysis depicted in Figure 5 and 6. Figure 8 which exhibits the R values obtained for all members in the scenario of hanging member rupture, attributable to corrosion. Members with R values surpassing 1.0, denoting the ultimate state. In Figure 5 and Figure 6 and Figure 9 depict the analysis under service loading conditions, five group members positioned within the same plane as the assumed failing member are simulated. The hanger member adjacent to the hypothesized failed member exhibits more R values which reaches a maximum R value of almost 1.0. This observation suggests a critical vulnerability wherein the entire bridge

could face imminent collapse due to a single set member failure. Conversely, in the scenarios where no active load is accounted for and the girder is modeled with pin connections, only one single line of members is removed from each upper and lower chord on the identical plane as the hypothetical hanger member attains the ultimate state and ruptures. These cases represent varying degrees of deterioration resulting from corrosion-induced damage to the hanging material, as illustrated in redundancy analysis in the preceding section meticulously scrutinized the load-bearing capacity of individual members, the evaluation showed if the section reaches an end state concurrent with member failure, the resulting damage propagation may lead to an entire system failure, diverging from the outcomes of the prior analysis.

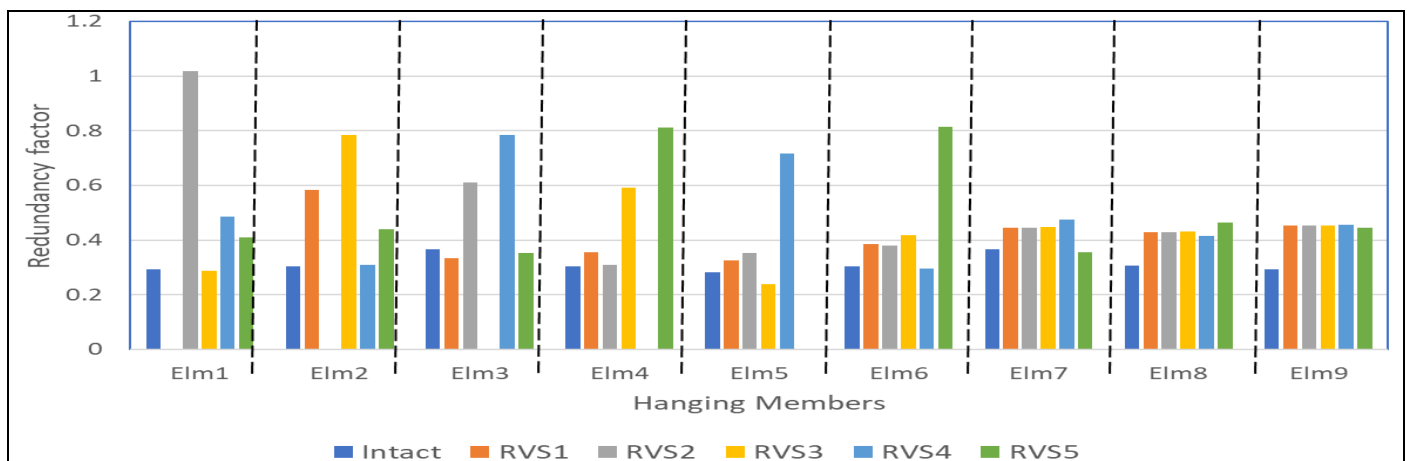
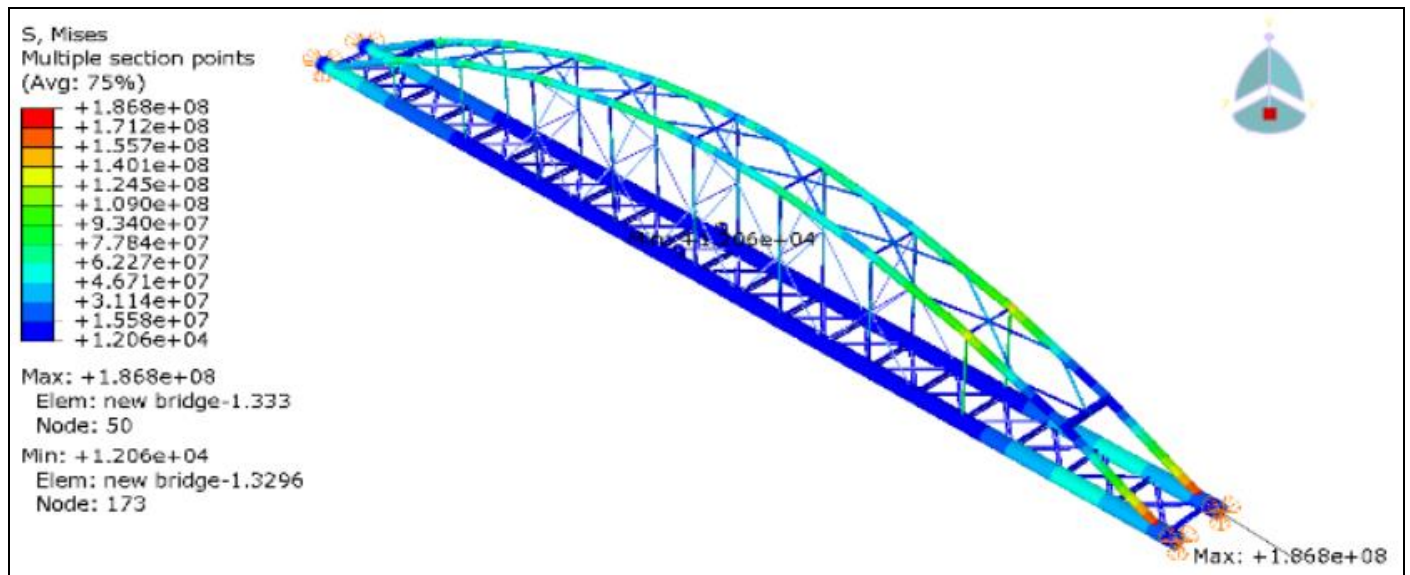
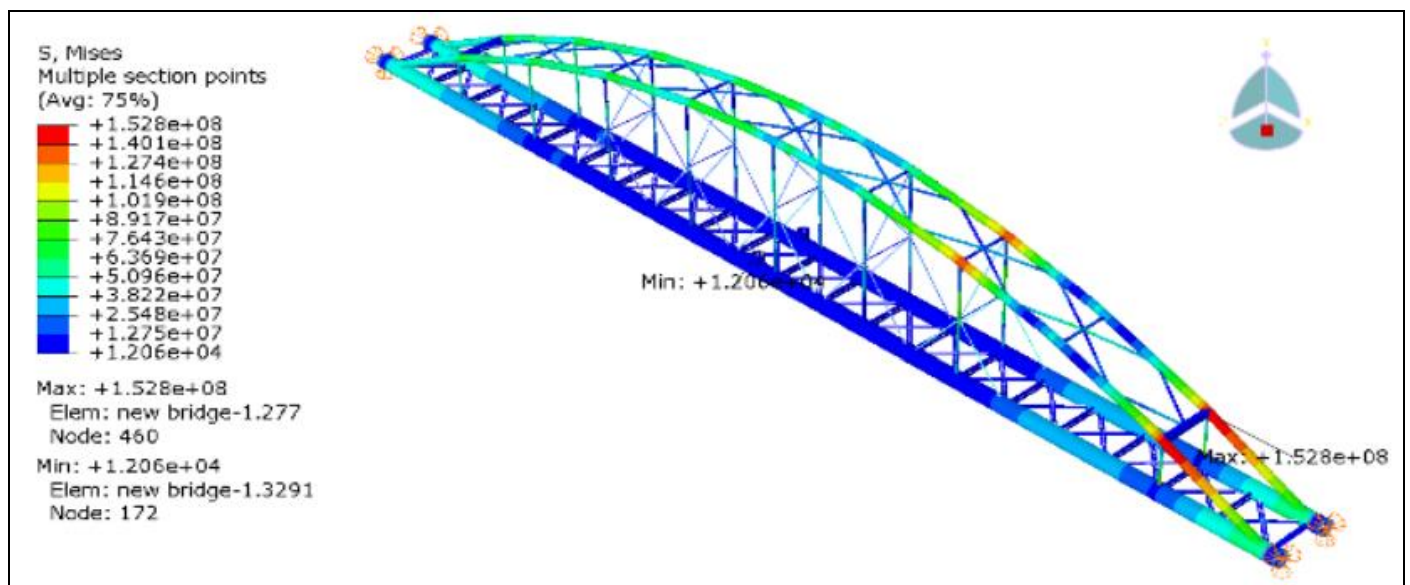


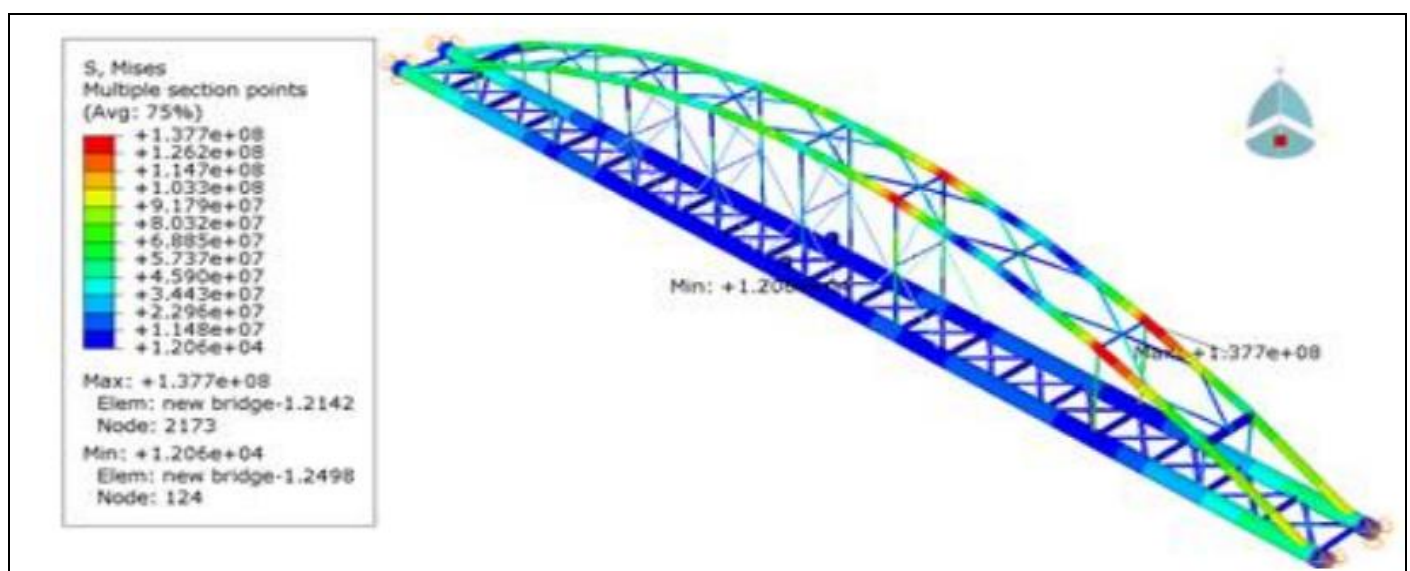
Fig 8 GenRedundancy factor where critical hanging members; Cases (a) to (e) are corroded



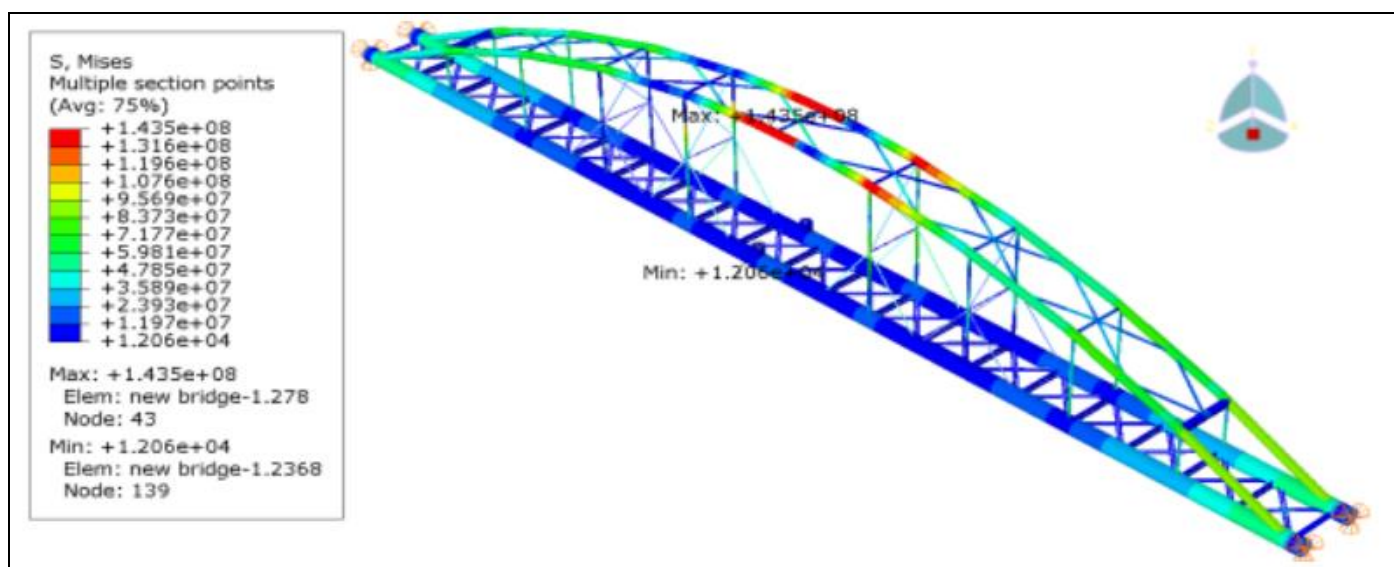
(a)



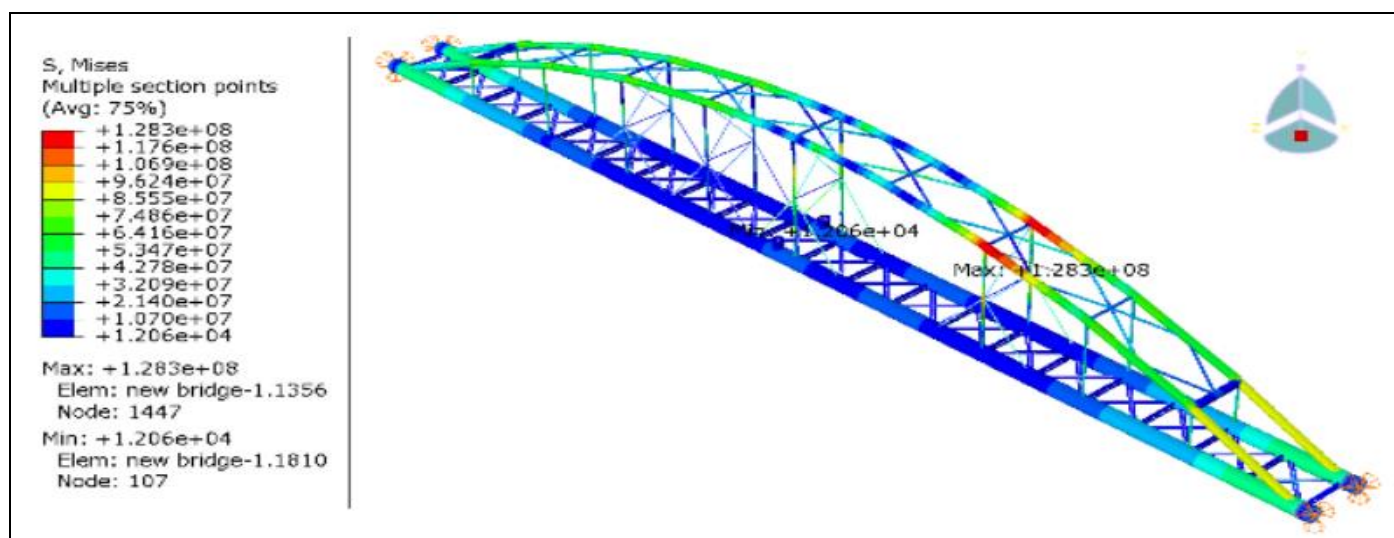
(b)



(c)



(d)



(e)

Fig 9 General view of stress distribution where critical hanging members; Cases (a) to (e) are corroded

VII. CONCLUSION

The synthesis of varied analyses undertaken on the Langer arch bridge elucidates several fundamental conclusions, elucidating crucial facets of its structural performance and redundancy. The examination of stress distribution in hangers across diverse scenarios demonstrates that the most extreme hangers endure the highest levels of stress within the Langer arch bridge. Specifically, the failure of hangers located near the supports intensifies stress on subsequent hangers, while failures at midspan lead to a more equitable redistribution of stresses. This differentiation indicates varying mechanisms of load path redistribution, manifesting as localized effects for edge hanger failures and more extensive effects for midspan hanger failures. In summation, the comprehensive analyses conducted offer valuable insights into the structural behavior and resilience of the Langer arch bridge, providing a foundation for informed decision-making in bridge design, maintenance, and risk management practices. These findings underscore the

imperative of integrating resilience considerations into infrastructure planning and highlight avenues for enhancing the robustness and longevity of critical bridge systems in the face of diverse challenges and threats.

REFERENCES

- [1]. F. Yamazaki, W. Liu, T. Furuya, and Y. Maruyama, "Assessment of Aqueduct Bridge Failure in Wakayama City, Japan, Based on Uav Surveying Flights and High-Resolution Sar Data," *Int. Geosci. Remote Sens. Symp.*, vol. 2022-July, pp. 497–500, 2022, doi: 10.1109/IGARSS46834.2022.9883792.
- [2]. K. Kinoshita, T. Kumura, Y. Yamaguchi, and T. Tanaka, "Anomalous Displacement Detection of Bridges Using Satellite SAR: A Case Study on a Collapse of Musota Water Pipe Bridge," *Int. Geosci. Remote Sens. Symp.*, vol. 2023-July, pp. 1720–1723, 2023, doi: 10.1109/IGARSS52108.2023.10283463.

- [3]. N. Mohammadi, Y. Kuwata, and A. Morioka, "Observation monitoring and modal analysis of aqueduct bridge considering corrosion: a case study of the Musota Aqueduct Bridge," *J. JSCE*, vol. 12, no. 2, pp. 23–13137, 2024, doi: 10.2208/JOURNALOFJSCE.23-13137.
- [4]. M. Ghosn and F. Moses, "NCHRP Report 406: Redundancy In Highway Bridge Superstructures," *Onlinepubs.Trb.Org*, p. 44, 1998.
- [5]. S. Hao, "I35W Bridge Collapse: Lessons Learned and Challenges Revealed," *Struct. Congr. 2011 - Proc. 2011 Struct. Congr.*, pp. 3153–3170, 2011, doi: 10.1061/41171(401)275.
- [6]. M. of Wakayama Office of River and National Highway and T. and T. Land, Infrastructure, Failure scene of an aqueduct bridge from a fixed-point camera, (2021).
- [7]. S.-S. Li, G.-Y. Sang, M.-Y. Xu, and Y. Ye, "Different Aqueduct Structure Make and Design," *Mater. Environ. Eng.*, pp. 1177–1184, Oct. 2017, doi: 10.1515/9783110516623-115/HTML.
- [8]. "API STD 1104: Welding of Pipelines and Related Facilities," vol. 22, 2021.
- [9]. L. K. Sing, S. N. A. Azraai, N. Yahaya, L. Zardasti, and N. Md Noor, "Strength development of epoxy grouts for pipeline rehabilitation," *J. Teknol.*, vol. 79, no. 1, 2017, doi: 10.11113/jt.v79.9339.
- [10]. M. Shamsuddoha, M. M. Islam, T. Aravinthan, A. Manalo, and K. tak Lau, "Effectiveness of using fibre-reinforced polymer composites for underwater steel pipeline repairs," 2013. doi: 10.1016/j.compstruct.2012.12.019.
- [11]. A. Diniță et al., "Advancements in Fiber-Reinforced Polymer Composites: A Comprehensive Analysis," 2024. doi: 10.3390/polym16010002.
- [12]. D. R. Mertz and U. S. F. H. A. O. of B. Technology, *Steel Bridge Design Handbook: Redundancy*. United States. Federal Highway Administration. Office of Bridge Technology, 2012. doi: 10.21949/1503647.
- [13]. D. M. Frangopol and J. P. Curley, "Effects of Damage and Redundancy on Structural Reliability," *J. Struct. Eng.*, vol. 113, no. 7, pp. 1533–1549, Jul. 1987, doi: 10.1061/(ASCE)0733-9445(1987)113:7(1533).
- [14]. Hazus, *Hazus–MH 2.1: Technical Manual*. 2012.
- [15]. Caltrans, "Memo to Designers 12-2: Guidelines for Identification of Steel Bridge Members.," 2012.
- [16]. R. Pekelnicky and C. Poland, "ASCE 41-13: Seismic Evaluation and Retrofit Rehabilitation of Existing Buildings," *Citeseer*, 2012, doi: 10.1016/j.aqpro.2013.07.003.